International Journal of Minerals, Metallurgy and Materials
Volume 25, Number 4, April 2018, Page 472
https://doi.org/10.1007/s12613-018-1593-8

Effect of TiO_2 nanoparticles on hydrogen evolution reaction activity of Ni coatings

Revanna Kullaiah, Liju Elias, and Ampar Chitharanjan Hegde

Electrochemistry Research Lab, Department of Chemistry, National Institute of Technology Karnataka, Srinivasnagar P. O., Surathkal, Mangalore-575025, India
(Received: 27 July 2017; revised: 30 November 2017; accepted: 8 December 2017)

Abstract: The electrocatalytic activity of electrodeposited Ni and Ni–TiO_2 coatings with regard to the alkaline hydrogen evolution reaction (HER) was investigated. The Ni coatings were electrodeposited from an acid chloride bath at different current densities, and their HER activities were examined in a 1.0-mol·L^{-1} KOH medium. The variations in the HER activity of the Ni coatings with changes in surface morphology and composition were examined via the electrochemical dissolution and incorporation of nanoparticles. Electrochemical analysis methods were used to monitor the HER activity of the test electrodes; this activity was confirmed via the quantification of gases that evolved during the analysis. The obtained results demonstrated that the Ni–TiO_2 nanocomposite test electrode exhibited maximum activity toward the alkaline HER. The surface appearance, composition, and the phase structure of all developed coatings were analyzed using scanning electron microscopy (SEM), energy dispersive spectroscopy (EDS), and X-ray diffraction (XRD), respectively. The improvement in the electrocatalytic activity of Ni–TiO_2 nanocomposite coating toward HER was attributed to the variation in surface morphology and increased number of active sites.

Keywords: coatings; electrodeposition; nanocomposite; electrocatalysis

1. Introduction

Hydrogen is considered as an alternative to fossil fuel because it is a clean and fully recyclable energy carrier [1–2]. The present global energy consumption provides evidence for the depletion of fossil fuel resources and the ever-increasing environmental pollution; owing to this, a more sustainable energy infrastructure needs to be developed [2]. Accordingly, the utilization of hydrogen as a primary energy carrier may contribute to a future with secure and clean energy infrastructure [3]. Water is the cheapest and most abundant source of hydrogen, and the ability to produce high purity hydrogen from water makes electrolysis of water a promising technique among many others [4–5]. The high energy consumption owing to the overpotential for hydrogen evolution reaction (HER) has constrained the widespread use of practical electrocatalysis applications [6]. However, the overpotential for electrocatalysis, which is mainly caused by the activation polarization, can be reduced up to a certain extent by modifying the electrode materials [7–8].

Electrodeposition is one of the most effective methods for the development of electroactive coatings [9–11]. A wide variety of materials with tailored properties can be inexpensively and efficiently synthesized via electrodeposition [12]. The electrodeposited alloys and composites were reported as efficient electrode materials for alkaline HER [13–15]. Composite electrodeposition is a rapidly growing research field. This method makes it possible to achieve the material characteristics that cannot be achieved using other methods [16]. The development of composite coatings with homogeneously dispersed nanoparticles can enhance the electrocatalytic activity of its metal/alloy counterparts [17–18]. The efficacy of Ni based metal, alloy, and composite coatings from various applications such as corrosion protection, electrocatalytic activity, and wear resistance has been reported [5,17,19]. Although Ni is not an active electrocatalytic material, its alloys and composites are considered as efficient electrocatalytic materials in the alkaline water

Corresponding author: Ampar Chitharanjan Hegde E-mail: acrhegde@gmail.com

splitting reaction [11,15,19–21]. Among the various reported nanocomposite coatings, TiO_2 based nanocomposite coatings exhibit better activity toward electrocatalysis and photocatalysis [11,21]. Advanced methods for the development of TiO_2 based nanocomposite thin films have been reported [22–23]. The nanocomposite coatings were developed using the composite electrodeposition method herein.

With consideration to the bright appearance and better corrosion resistance of the Ni coatings, an effort was made to enhance their electrocatalytic character via electrochemical anodic dissolution and TiO_2 nanoparticle incorporation.

2. Experimental

2.1. Deposition of Ni coatings

The Ni coatings were deposited from an acid chloride bath optimized by Hull-cell with $NiCl_2{\cdot}6H_2O$ (131.2 $g{\cdot}L^{-1}$), NH_4Cl (25 $g{\cdot}L^{-1}$), H_3BO_3 (20 $g{\cdot}L^{-1}$), and $C_3H_8O_3$ (1.0 $g{\cdot}L^{-1}$). All the chemicals were procured from Merck, Mumbai, and the plating bath was prepared by dissolving the chemicals in double distilled water. The pH value of plating bath was maintained at 3.5 using HCl and NaOH. The coatings were developed on the pre-cleaned copper rod of unit surface area using a homemade electrodeposition setup with a capacity of 400 mL (Fig. 1). The depositions were performed galvanostatically at different current densities (C.Ds) such as 1.0, 3.0, and 5.0 $A{\cdot}dm^{-2}$ using a DC power source (Agilent N6705A, Agilent Technologies, USA).

The electrochemical anodic dissolution or selective leaching of the as-deposited Ni coating was performed to investigate the variation of the HER activity of coatings as a result of introducing porosity to the surface. For comparison, the Ni coatings deposited at 3.0 $A{\cdot}dm^{-2}$, which showed the best performance toward the alkaline HER, was selected for the dissolution. The electrochemical dissolution of the as-coated sample was performed in a dissolution medium of 0.1 $mol{\cdot}L^{-1}$ HNO_3. The dissolution time and C.D. were optimized for the better performance of the coatings with regard to HER. The experimental results revealed that dissolution for 3 min at a C.D. of 1.0 $A{\cdot}dm^{-2}$ had an enhancing effect on the performance of the coatings.

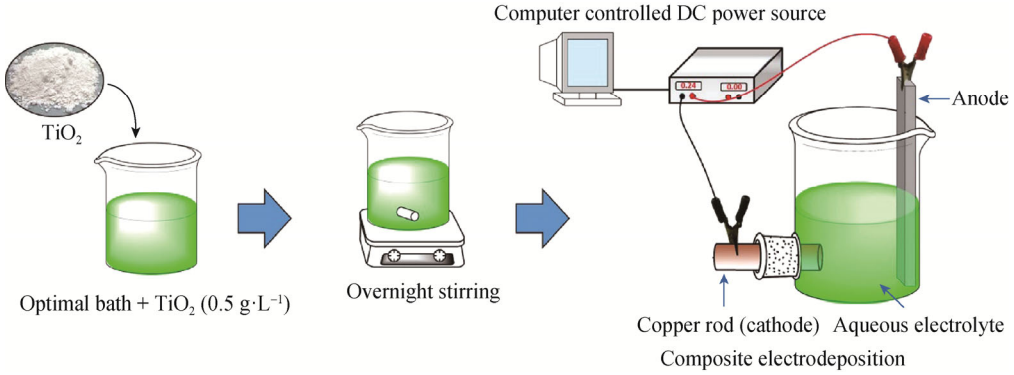

Fig. 1. Schematic of composite electrodeposition in homemade electrodeposition setup with 400 mL capacity.

2.2. Electrodeposition of Ni–TiO_2 nanocomposite coatings

The Ni–TiO_2 nanocomposite coatings was developed from the same optimal Ni plating bath loaded with homogeneously dispersed TiO_2 nanoparticles (0.5 $g{\cdot}L^{-1}$). The TiO_2 nanoparticles (particle size < 25 nm, anatase) used in the present study were procured from Sigma-Aldrich Company, St. Louis, MO, USA, and used directly. The best obtained C.D. for the deposition of Ni coatings (3.0 $A{\cdot}dm^{-2}$) was selected for developing the nanocomposite coatings. All the metal and composite depositions were performed for the same time duration (600 s). Fig. 1 schematizes the composite electrodeposition.

2.3. Characterization of electrodeposited coatings

The surface appearance, composition, and phase structure of the metal coatings, dissoluted sample, and nanocomposite coatings were examined using a scanning electron microscope (SEM, JSM–7610F, JEOL, USA), energy dispersive spectroscopy (EDS, Link ISIS-300 micro-analytical system, Oxford Instruments, UK), and X-ray diffraction (XRD, JEOL JDX-8P0), respectively. Furthermore, the thickness of the deposits was calculated using Faraday's law and verified using a digital thickness tester (Coatmeasure M&C, ISO–17025). The hardness of the deposits was measured with a microhardness tester (CLEMEX, CMT. HD, Canada) using the Vickers method. The electrochemical characteristics of the developed coatings toward the HER were examined in a medium of 1.0-$mol{\cdot}L^{-1}$ KOH using a custom-made three-electrode glass setup, as reported in our earlier studies [9,15]. The saturated calomel electrode (SCE)

and platinum electrode were used as the reference and counter electrodes, respectively, in the three-electrode cell. Electrochemical techniques such as cyclic voltammetry (CV) and chronopotentiometry (CP) were used to test the electrocatalytic efficiency of test electrodes toward the alkaline HER. Moreover, the practical activity of the test electrodes was confirmed from the quantification of gases that evolved during the analysis. The CV was performed in a potential window of 0 to −1.6 V at a scan rate of 50 $mV \cdot s^{-1}$ for 50 cycles. The onset potential and cathodic peak current density (i_{pc}) for HER were observed from the recorded "*i*–*V*" curves. The CP analysis was performed at a constant C.D. of −300 $mA \cdot cm^{-2}$ for a duration of 1800 s, and the amount of H_2 gas that evolved during the analysis was quantified.

3. Results and discussion

3.1. Electrodeposited Ni coatings

The effect of the deposition C.D. on coating characteristics such as the nature of deposit, coating thickness, and microhardness are listed in Table 1. The coatings deposited at 1.0 and 3.0 $A \cdot dm^{-2}$ were visually inspected and observed to be bright. However, the coatings developed at 5.0 $A \cdot dm^{-2}$ were observed to be semi-bright with powdery appearance. Although the thickness of the coatings was observed to increase with the increase in deposition C.D., the microhardness values increased only up to a deposition C.D. of 3.0 $A \cdot dm^{-2}$ and then decreased. The decrease in the microhardness value for the coating obtained at 5.0 $A \cdot dm^{-2}$ compared with the coating at 3.0 $A \cdot dm^{-2}$ may be attributed to the powdery nature of the deposit at 5.0 $A \cdot dm^{-2}$.

3.2. XRD study

The variation in the phase structure of Ni coatings with deposition C.D. was analyzed using XRD; the XRD patterns were obtained for the Ni coatings deposited at 1.0, 3.0, and 5.0 $A \cdot dm^{-2}$ and are shown in Fig. 2. All the deposited Ni coatings were observed to have (111), (200), (220), and (311) reflections, which indicated the face centered cubic structure [19–20]. The intensity of the reflections was observed to increase with the deposition C.D., as shown in Fig. 2. When the deposition C.D. was increased from 1 $A \cdot dm^{-2}$ to 5 $A \cdot dm^{-2}$, the grain size of the coatings was also found to be increased from 21 to 34 nm.

Table 1. Effect of deposition C.D. on the coating characteristics of electrodeposited Ni coatings

Deposition C.D. / ($A \cdot dm^{-2}$)	Thickness / μm	Vickers microhardness, V_{100} / GPa	Nature of the deposit
1.0	6.1	1.2	Bright
3.0	9.6	1.7	Bright
5.0	11.9	1.5	Semi-bright

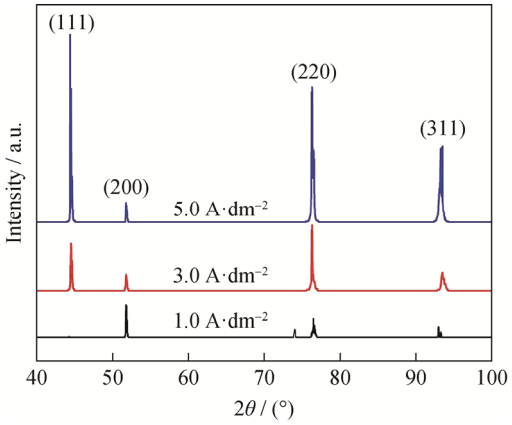

Fig. 2. XRD patterns of Ni coatings developed at different C.Ds from the same bath.

3.3. SEM study

The surface morphology of Ni coatings deposited from the optimal bath was investigated via SEM analysis. The Ni deposits obtained at different C.Ds were compact and composed of tiny grains covering the entire surface, as shown in Fig. 3. The variation in the surface appearance of the coatings with deposition C.D. (Fig. 3) implied the dependence of deposition C.D. on the characteristics of coatings. The microstructure of the Ni deposit achieved at 5.0 $A \cdot dm^{-2}$ was observed to be eutectic and had dendritic grains with non-uniform grain size distribution, as shown in Fig. 3(c).

3.4. HER activity of Ni coatings

The electrocatalytic activity of the Ni coatings toward alkaline HER was investigated in 1.0-$mol \cdot L^{-1}$ KOH medium using the CV and CP techniques.

3.4.1. CV study

The cyclic voltammograms were recorded to investigate the current response characteristics of the test electrodes (Ni coatings) within the potential (*E*) range. The activity of the

materials toward HER was assessed from CV characteristics such as cathodic peak current density (i_{pc}) and onset potential [10–12]. The obtained CV responses of the test electrodes developed at different C.Ds are shown in Fig. 4, and the corresponding i_{pc} and the onset potential values are listed in Table 2. The obtained results suggest that the best coating was developed at 3.0 A·dm^{-2}, with a minimum onset potential and maximum i_{pc} value.

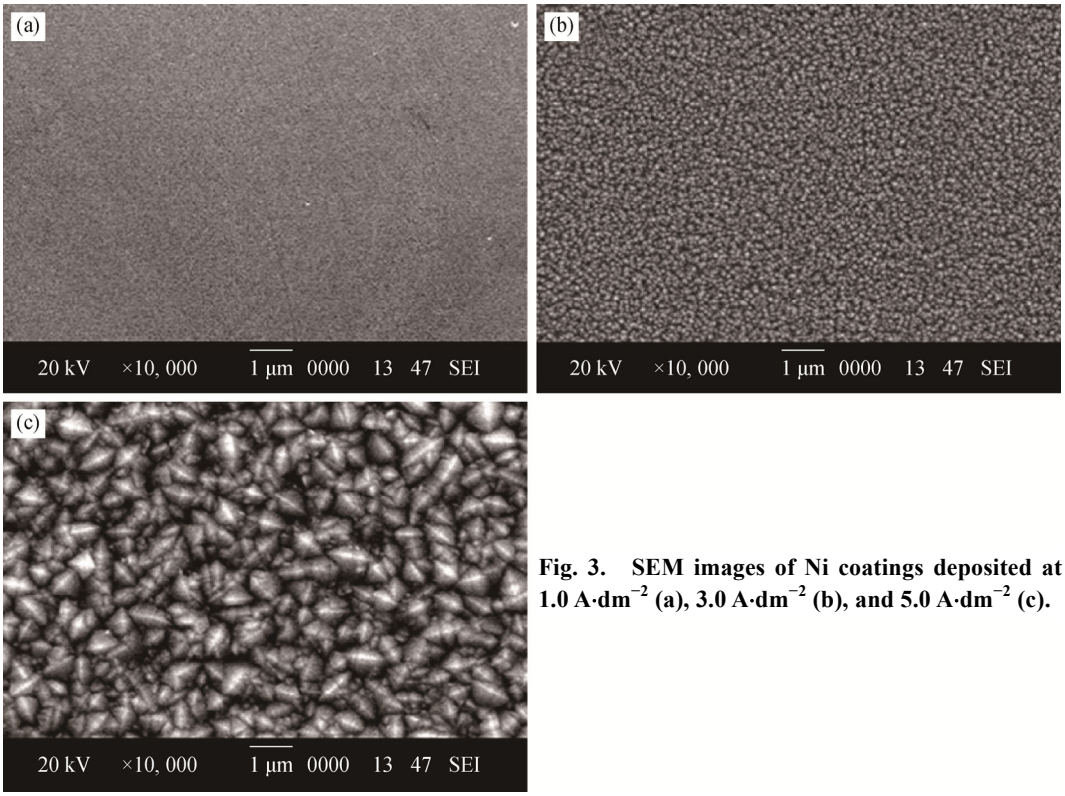

Fig. 3. SEM images of Ni coatings deposited at 1.0 A·dm^{-2} (a), 3.0 A·dm^{-2} (b), and 5.0 A·dm^{-2} (c).

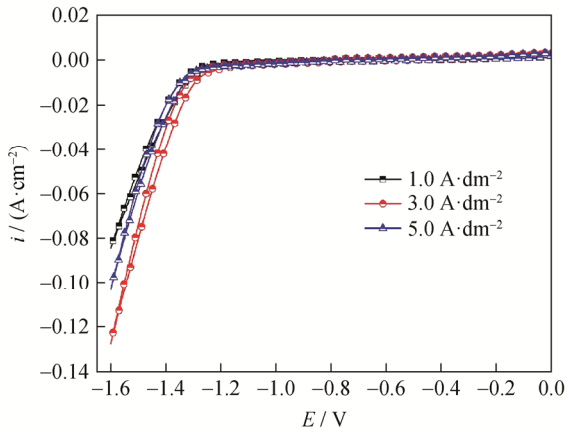

Fig. 4. CV responses of the Ni coatings developed at different C.Ds showing a variation in cathodic peak current density.

3.4.2. Chronopotentiometry study

The HER activity of the Ni coatings was monitored using CP, which is a simple electrochemical method. In this method, the potential response of the test electrode was monitored while passing a constant current between two electrodes as a function of time with respect to a suitable reference electrode [11]. The basis of the controlled current experiments was redox (electron transfer) reactions that must occur at the surface of the working electrode to support the applied current. To directly correlate the practical performance of the deposits to the electrochemical data, the amount of H_2 gas that evolved during the analysis was also measured (Table 2).

The CP responses and amount of H_2 liberated in the first 300 s from each Ni coating are shown in Fig. 5. The Ni coating achieved at 3.0 A·dm^{-2} produced the maximum

Table 2. HER parameters of Ni coatings developed at different C.Ds from optimal bath

Coating	Cathodic peak C.D. at –1.6 V / (A·cm^{-2})	Onset potential of H_2 evolution / V vs. SCE	Volume of H_2 evolved in 300 s / mL
Developed at 1.0 A·dm^{-2}	–0.085	–1.33	8.9 ± 0.2
Developed at 3.0 A·dm^{-2}	–0.126	–1.24	11.9 ± 0.2
Developed at 5.0 A·dm^{-2}	–0.102	–1.28	10.2 ± 0.1

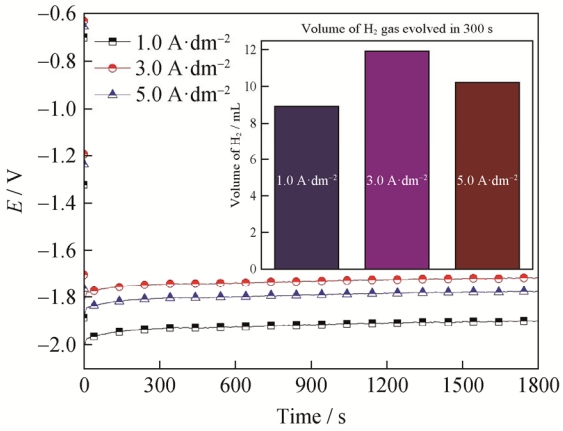

Fig. 5. CP curves for Ni coatings under impressed cathodic current of −300 mA·cm^{-2} along with the volume of H_2 gas evolved over 300 s on each test electrode (at the inset).

amount of H_2 gas (11.9 mL) compared to the other coatings deposited at 1.0 and 5.0 A·dm^{-2}, confirming that the Ni coating obtained at 3.0 A·dm^{-2} was the best material with regard to the HER. In comparison to the coatings developed at other C.Ds, the increased HER activity and electrochemical stability of the coating developed at 3.0 A·dm^{-2} may be attributed to its physical stability, which was confirmed from the microhardness value.

3.5. Modified Ni coatings for alkaline HER

The Ni coating deposited at 3.0 A·dm^{-2}, which was observed to have maximum activity toward alkaline HER, was selected for further modification. The coating was modified via the electrochemical dissolution and incorporation of TiO_2 nanoparticles. The obtained porous Ni coating and Ni–TiO_2 nanocomposite coating were tested for their electrocatalytic activity toward alkaline HER.

3.6. SEM analysis of porous Ni coating

The electrochemical anodic dissolution or selective leaching of the as-deposited Ni coating was performed to investigate the improvement of the metal coating's electrocatalytic behavior resulting from the introduction of porosity to the surface. The formation of the porous coating after the dissolution treatment is shown in Fig. 6. The SEM image clearly shows similar variations in the surface morphology of the coating after the dissolution treatment, as reported by Islam and Shehbaz [24]. The increased surface area of the sample after leaching was attributed to the presence of micropores and nanopores on the coating surface [11].

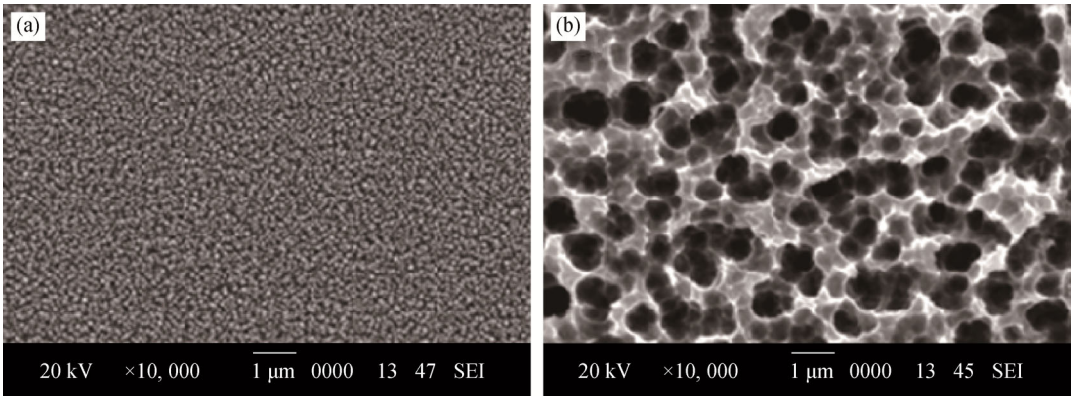

Fig. 6. SEM images of Ni coatings deposited at 3.0 A·dm^{-2} before dissolution (a) and after dissolution (b).

3.7. SEM analysis of Ni–TiO_2 nanocomposite coating

The morphological variation of the Ni coating after the incorporation of TiO_2 nanoparticles was investigated via SEM analysis, whereas the presence of TiO_2 nanoparticles in the coating was confirmed via EDS analysis. The comparison of the obtained SEM nanocomposite coating image of the Ni coating and the EDS result of the composite coating are shown in Fig. 7(c). The amount of TiO_2 nanoparticles incorporated in the coating was approximately 4.2wt%. The metal deposition rate increased at sites wherein the nanoparticles were incorporated into the metal matrix, thereby increasing the total surface roughness.

3.8. Electrocatalytic activity of modified Ni coatings toward HER

3.8.1. CV investigation

The HER activity of the modified Ni coatings was investigated via CV analysis, as it has been done for the conventional Ni coatings. The onset potential and i_{pc} values for the modified test electrodes were noted from the stable and reproducible cycles of the obtained CV curves and are shown in Fig. 8. The Ni coating was observed to determine the improvement in HER activity after the electrochemical dissolution and

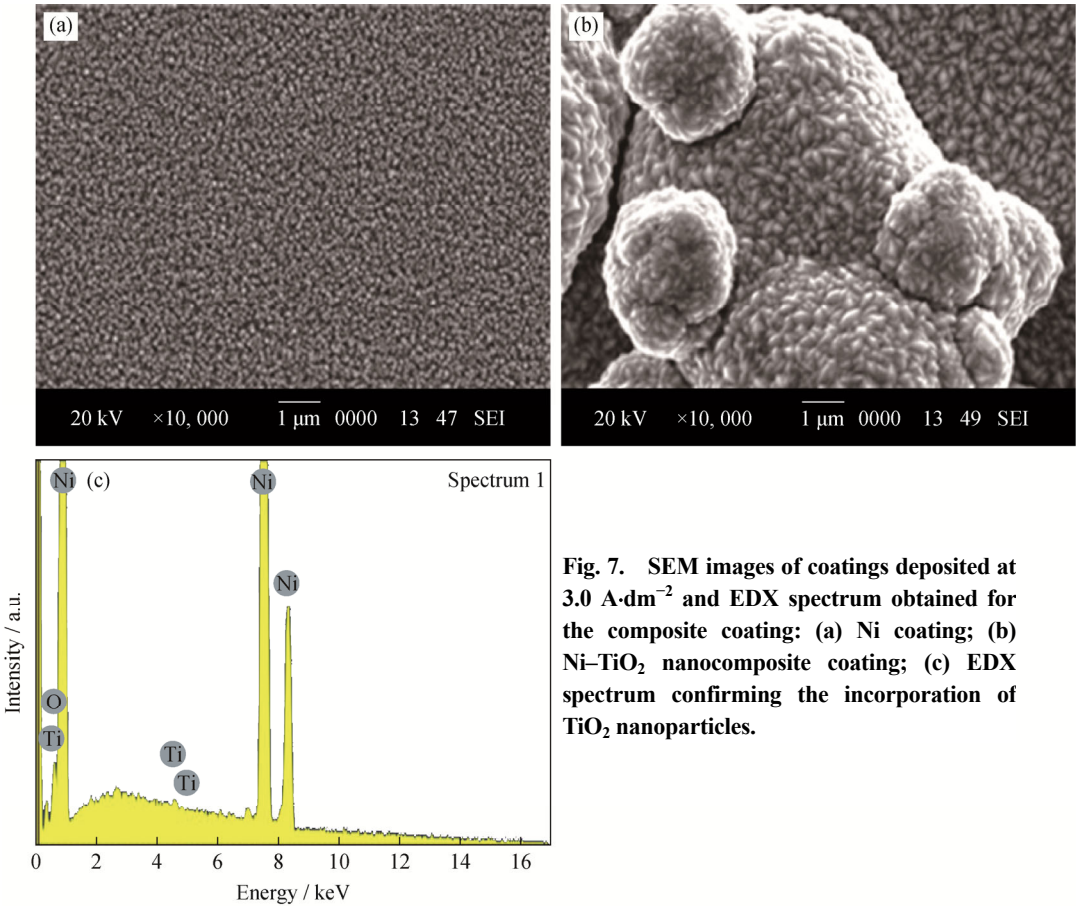

Fig. 7. SEM images of coatings deposited at 3.0 A·dm^{-2} and EDX spectrum obtained for the composite coating: (a) Ni coating; (b) Ni–TiO_2 nanocomposite coating; (c) EDX spectrum confirming the incorporation of TiO_2 nanoparticles.

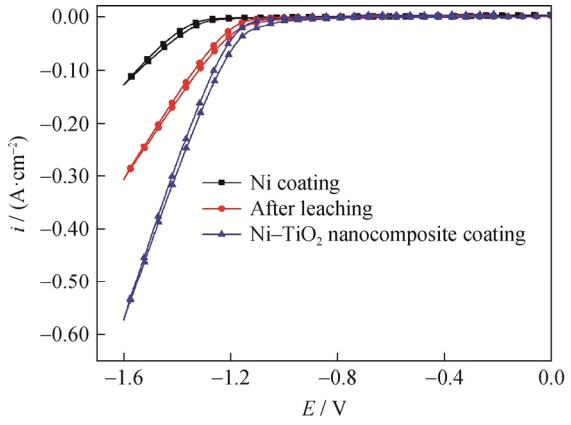

Fig. 8. CV responses of modified Ni coatings in comparison to conventional Ni coating.

incorporation of TiO_2 nanoparticles. The variation in electrocatalytic efficiency toward HER was evident from the i_{pc} and onset potential values listed in Table 3. The obtained CV responses confirmed that the Ni–TiO_2 nanocomposite coating was the most suitable coating for alkaline HER.

3.8.2. Chronopotentiometry study

The HER efficiency variation after the dissolution and incorporation of the TiO_2 nanoparticles was confirmed via the CP responses of the modified Ni electrodes. The CP responses and the evolved amount of H_2 gas are shown in Fig. 9, and the corresponding parameters are listed in Table 3. The CP analysis also confirmed that the Ni–TiO_2 nanocomposite was the best material for alkaline HER with the maximum amount of evolved H_2 gas.

Table 3. HER parameters of modified Ni coatings in comparison to conventional Ni coating under same working conditions

Coating type (deposited at 3.0 A·dm^{-2})	Cathodic peak C.D. at –1.6 V / (A·cm^{-2})	Onset potential of H_2 evolution / V vs. SCE	Volume of H_2 evolved in 300 s / cm^3
Ni coating	–0.126	–1.24	11.9 ± 0.2
Ni coating after dissolution	–0.30	–1.20	13.6 ± 0.1
Ni–TiO_2	–0.57	–1.02	16.1 ± 0.1

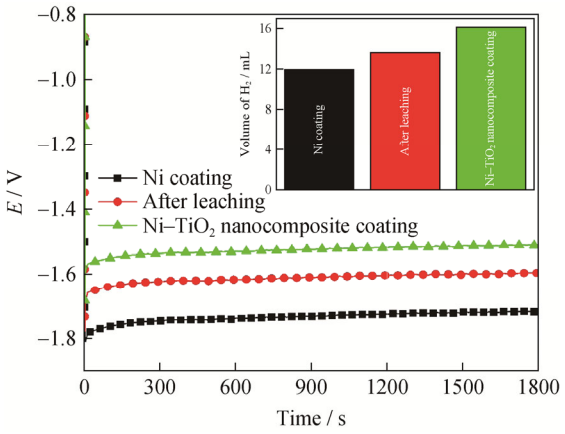

Fig. 9. Comparison of CP curves for modified Ni coatings to conventional Ni coating, and volume of H_2 gas evolved on each test electrode (at inset).

The variation in the electrocatalytic efficiency of Ni coating after leaching and the incorporation of TiO_2 nanoparticles was attributed to the increase in the effective surface area and number of electroactive sites and was achieved using modification techniques [15,25]. The micro/nanopores introduced on the coating surface after the anodic dissolution increased the surface area as more active metal sites were exposed [11]. However, in the case wherein nanocomposite coating was used, the enhancement of HER activity was attributed to the incorporated electroactive TiO_2 nanoparticles. The electrochemical stability and activity of the composite coatings are in agreement with the results that have been reported in the literature [26]. The incorporation of TiO_2 nanoparticles led to the increase of the effective surface area and number of electroactive sites, thereby enhancing the HER activity [11,15].

4. Conclusions

The following conclusions were drawn from the detailed analysis of the experimental results obtained from the HER investigation on Ni and modified Ni coatings.

(1) Ni coating deposited at 3.0 $A \cdot dm^{-2}$ was determined as efficient electrode materials for HER, and this was demonstrated via CV and CP experiments.

(2) The electrochemical dissolution of the coating toward the peak performance of HER was optimized without losing the stability of the electrode under working conditions.

(3) A novel electrodeposited Ni–TiO_2 nanocomposite coating was reported as an efficient electrocatalytic material for the HER.

(4) The electrocatalytic efficiency of Ni electrodes was improved significantly by the incorporation of TiO_2 nanoparticles on the developed coating.

Acknowledgement

Dr. Liju Elias is thankful to National Institute of Technology Karnataka (NITK), Surathkal, India, for providing the facilities to conduct this research.

References

[1] T.N. Veziroğlu and S. Şahin, 21st century's energy: hydrogen energy system, *Energy Convers. Manage.*, 49(2008), No. 7, p. 1820.

[2] T.N. Veziro» lu and F. Barbir, Hydrogen: the wonder fuel, *Int. J. Hydrogen Energy*, 17(1992), No. 6, p. 391.

[3] X.X. Zou and Y. Zhang, Noble metal-free hydrogen evolution catalysts for water splitting, *Chem. Soc. Rev.*, 44(2015), No. 15, p. 5148.

[4] D. Pletcher, Electrocatalysis: present and future, *J. Appl. Electrochem.*, 14(1984), No. 4, p. 403.

[5] F. Safizadeh, E. Ghali, and G. Houlachi, Electrocatalysis developments for hydrogen evolution reaction in alkaline solutions—A review, *Int. J. Hydrogen Energy*, 40(2015), No. 1, p. 256.

[6] D. Pletcher and X.H. Li, Prospects for alkaline zero gap water electrolysers for hydrogen production, *Int. J. Hydrogen Energy*. 36(2011), No. 23, p. 15089.

[7] B.V. Tilak, A.C. Ramamurthy, and B.E. Conway, High performance electrode materials for the hydrogen evolution reaction from alkaline media, *J. Chem. Sci.*, 97(1986), No. 3-4, p. 359.

[8] D.S.P. Cardoso, L. Amaral, D.M.F. Santos, B. Šljukić, C.A.C. Sequeira, D. Macciò, and A. Saccone, Enhancement of hydrogen evolution in alkaline water electrolysis by using nickel-rare earth alloys, *Int. J. Hydrogen Energy*, 40(2015), No. 12, p. 4295.

[9] L.J. Elias, K. Scott, and A.C. Hegde, Electrolytic synthesis and characterization of electrocatalytic Ni–W alloy, *J. Mater. Eng. Perform.*, 24(2015), No. 11, p. 4182.

[10] L. Elias, P. Cao, and A.C. Hegde, Magnetoelectrodeposition of Ni–W alloy coatings for enhanced hydrogen evolution reaction, *RSC Adv.*, 6(2016), No. 112, p. 111358.

[11] L. Elias and A.C. Hegde, Modification of Ni–P alloy coatings for better hydrogen production by electrochemical dissolution and TiO_2 nanoparticles, *RSC Adv.*, 6(2016), No. 70, p. 66204.

[12] N. Kanani, *Electroplating: Basic Principles, Processes and Practice*, Elsevier, Germany, 2004, p. 5.

[13] L. Beneaand and A.I. Pavlov, Ni–TiO_2 nanocomposite coatings as cathode material for hydrogen evolution reaction, *J. Optoelectron. Adv. Mater.*, 7(2013), No. 11-12, p. 895.

[14] P. Baghery, M. Farzam, A.B. Mousavi, and M. Hosseini, Ni–TiO_2 nanocomposite coating with high resistance to cor-

rosion and wear, *Surf. Coat. Technol.*, 204(2010), No. 23, p. 3804.

[15] L. Elias and A.C. Hegde, Synthesis and characterization of Ni–P–Ag composite coating as efficient electrocatalyst for alkaline hydrogen evolution reaction, *Electrochim. Acta*, 219(2016), p. 377.

[16] C.T.J. Low, R.G.A. Wills, and F.C. Walsh, Electrodeposition of composite coatings containing nanoparticles in a metal deposit, *Surf. Coat. Technol.*, 201(2006), No. 1-2, p. 371.

[17] A.A. Aal and H.B. Hassan, Electrodeposited nanocomposite coatings for fuel cell application, *J. Alloys Compd.*, 477(2009), No. 1-2, p. 652.

[18] I.A. Raj, Nickel-based, binary-composite electrocatalysts for the cathodes in the energy-efficient industrial production of hydrogen from alkaline-water electrolytic cells, *J. Mater. Sci.*, 28(1993), No. 16, p. 4375.

[19] C.Q. Li, X.H. Li, Z.X. Wang, and H.J. Guo, Nickel electrodeposition from novel citrate bath, *Trans. Nonferrous Met. Soc. China*, 17(2007), No. 6, p. 1300.

[20] E. Rudnik, M. Wojnicki, and G. Włoch, Effect of gluconate addition on the electrodeposition of nickel from acidic baths, *Surf. Coat. Technol.*, 207(2012) 375.

[21] D. Gierlotka, E. Ro´winski, A. Budniok, and E.L. Giewka, Production and properties of electrolytic Ni–P–TiO_2 composite layers, *J. Appl. Electrochem.*, 27(1997), No. 12, p. 1349.

[22] I. Ruzybayev, E. Yassitepe, A. Ali, A.S. Bhatti, R.M. Mohamed, M. Islam, and S.I. Shah, Reactive pulsed laser deposited N–C codoped TiO_2 thin films, *Mater. Sci. Semicond. Process.*, 39(2015), p. 371.

[23] S. Javed, M. Mujahid, M. Islam, and U. Manzoor, Morphological effects of reflux condensation on nanocrystalline anatase gel and thin films, *Mater. Chem. Phys.*, 132(2012), No. 2-3, p. 509.

[24] M. Islam and T. Shehbaz, Effect of synthesis conditions and post-deposition treatments on composition and structural morphology of medium-phosphorus electroless Ni–P films, *Surf. Coat. Technol.*, 205(2011), No. 19, p. 4397.

[25] L. Elias and A.C. Hegde, Effect of including the carbon nanotube and graphene oxide on the electrocatalytic behavior of the Ni–W alloy for the hydrogen evolution reaction, *New J. Chem.*, 41(2017), No. 22, p. 13912.

[26] M. Islam, M.R. Azhar, N. Fredj, and T.D. Burleigh, Electrochemical impedance spectroscopy and indentation studies of pure and composite electroless Ni–P coatings, *Surf. Coat. Technol.*, 236(2013), p. 262.